



HAL
open science

High-Resolution Subspace-Based Methods: Eigenvalue- or Eigenvector-Based Estimation?

Konstantin Usevich, Souleymen Sahnoun, Pierre Comon

► **To cite this version:**

Konstantin Usevich, Souleymen Sahnoun, Pierre Comon. High-Resolution Subspace-Based Methods: Eigenvalue- or Eigenvector-Based Estimation?. LVA/ICA 2017 - 13th International Conference on Latent Variable Analysis and Signal Separation, Feb 2017, Grenoble, France. pp.47-56, 10.1007/978-3-319-53547-0_5 . hal-01576895

HAL Id: hal-01576895

<https://hal.science/hal-01576895>

Submitted on 24 Aug 2017

HAL is a multi-disciplinary open access archive for the deposit and dissemination of scientific research documents, whether they are published or not. The documents may come from teaching and research institutions in France or abroad, or from public or private research centers.

L'archive ouverte pluridisciplinaire **HAL**, est destinée au dépôt et à la diffusion de documents scientifiques de niveau recherche, publiés ou non, émanant des établissements d'enseignement et de recherche français ou étrangers, des laboratoires publics ou privés.

High-resolution subspace-based methods: eigenvalue- or eigenvector-based estimation?*

Konstantin Usevich**, Souleymen Sahnoun, and Pierre Comon

GIPSA-lab, CNRS and Univ. Grenoble Alpes, F-38000 Grenoble, France.
firstname.lastname@gipsa-lab.fr

Abstract. In subspace-based methods for multidimensional harmonic retrieval, the modes can be estimated either from eigenvalues or eigenvectors. The purpose of this study is to find out which way is the best. We compare the state-of-the-art methods N-D ESPRIT and IMDF, propose a modification of IMDF based on least-squares criterion, and derive expressions of the first-order perturbations for these methods. The theoretical expressions are confirmed by the computer experiments.

Keywords: Frequency estimation, multidimensional harmonic retrieval, multilevel Hankel matrix, N-D ESPRIT, IMDF, perturbation analysis.

1 Introduction

Parameter estimation from bidimensional (2-D) and multidimensional (N -D) signals finds many applications in signal processing and communications such as magnetic resonance (NMR) spectroscopy [5], wireless communication channel estimation, antenna array processing, radar and medical imaging [1]. In these applications, signals are modeled by a superposition of damped or undamped N -D complex exponentials.

Signal model. Denote N the number of dimensions and M_n , $n = 1, \dots, N$, the size of the sampling grid in each dimension. In this paper we consider the following model, for $m_n = 0, \dots, M_n - 1$:

$$\tilde{y}(m_1, \dots, m_N) = y(m_1, \dots, m_N) + \varepsilon(m_1, \dots, m_N), \quad (1)$$

where $\varepsilon(\cdot)$ is random noise (we leave the assumptions on the noise for later), and the signal y is a superposition of R N -D damped complex sinusoids:

$$y(m_1, \dots, m_N) = \sum_{r=1}^R c_r \prod_{n=1}^N (a_{r,n})^{m_n}, \quad (2)$$

where

* This work is funded by the European Research Council under the Seventh Framework Programme FP7/2007–2013 Grant Agreement no. 320594.

** Corresponding author.

- c_r are complex amplitudes,
- $a_{r,n} = e^{-\alpha_{r,n} + j\omega_{r,n}}$ are modes in the n -th dimension,
- $\{\alpha_{r,n}\}_{r=1,n=1}^{R,N}$ are (real and positive) damping factors,
- $\{\omega_{r,n} = 2\pi\nu_{r,n}\}_{r=1,n=1}^{R,N}$ are angular frequencies.

The problem is to estimate $\{a_{r,n}\}_{r=1}^R$ and $\{c_r\}_{r=1}^R$ from the observed signal $\tilde{y}(m_1, \dots, m_N)$.

State of art. To deal with this problem, several methods have been proposed. They include linear prediction-based methods such as 2-D TLS-Prony [10], and subspace approaches such as matrix enhancement and matrix pencil (MEMP) [3], 2-D ESPRIT [8], improved multidimensional folding (IMDF) [7,6], Tensor-ESPRIT [2], principal-singular-vector utilization for modal analysis (PUMA) [14,13]. Among the most promising are N-D ESPRIT [8,12] and IMDF [7,6]. Both methods use the eigenvalue decomposition (EVD) of a so-called shift matrix constructed from the estimated basis of the signal subspace, but the modes are extracted differently: from eigenvalues in ND-ESPRIT and from eigenvectors in IMDF. Which method is the best? To our knowledge, there is no satisfactory answer to this question in the literature. The purpose of this paper is to shed some light on this question.

Contributions. In this paper, we perform a study to compare between methods that are based on eigenvalues and those based on eigenvectors to extract N-D modes. Our main contributions are:

- We derive simple expressions of first-order perturbations of IMDF that do not need to calculate the SVD of the MH matrix as it is needed in expressions given in [6].
- We propose a variation of IMDF in which the modes are estimated by minimizing the least squares criterion. It is shown through perturbation analysis and simulations that the proposed technique outperforms the original average-base technique.

Organisation of the paper In Section 2, we recall the definition of multilevel Hankel (MH) matrices and their main properties. In Section 3, we recall the algorithms N-D ESPRIT and IMDF, and describe a proposed modification of IMDF (IMDF LS). In Section 4, we recall known results on first order perturbations and derive new expressions for IMDF and IMDF LS. Section 5 contains numerical experiments.

2 Multilevel Hankel matrices and their subspaces

2.1 Definition and factorization

Assume that the set of parameters $(L_n)_{n=1}^N$ is chosen such that $1 \leq L_n \leq M_n$ and define $K_n \stackrel{\text{def}}{=} M_n - L_n + 1$. The multilevel Hankel (MH) matrix $\mathbf{H} \in$

$\mathbb{C}^{(L_1 \cdots L_N) \times (K_1 \cdots K_N)}$ is defined as

$$\mathbf{H} = \begin{bmatrix} \mathbf{H}_0 & \mathbf{H}_1 & \cdots & \mathbf{H}_{K_1-1} \\ \mathbf{H}_1 & \mathbf{H}_2 & \cdots & \mathbf{H}_{K_1} \\ \vdots & \vdots & & \vdots \\ \mathbf{H}_{L_1-1} & \mathbf{H}_{L_1} & \cdots & \mathbf{H}_{M_1-1} \end{bmatrix}, \quad (3)$$

where for $n = 1, \dots, N-1$ the block matrices $\mathbf{H}_{m_1, \dots, m_n}$ are defined recursively

$$\mathbf{H}_{m_1, \dots, m_n} = \begin{bmatrix} \mathbf{H}_{m_1, \dots, m_n, 0} & \mathbf{H}_{m_1, \dots, m_n, 1} & \cdots & \mathbf{H}_{m_1, \dots, m_n, K_{r+1}-1} \\ \mathbf{H}_{m_1, \dots, m_n, 1} & \mathbf{H}_{m_1, \dots, m_n, 2} & \cdots & \mathbf{H}_{m_1, \dots, m_n, K_{r+1}} \\ \vdots & \vdots & & \vdots \\ \mathbf{H}_{m_1, \dots, m_n, L_{r+1}-1} & \mathbf{H}_{m_1, \dots, m_n, L_{r+1}} & \cdots & \mathbf{H}_{m_1, \dots, m_n, M_{r+1}-1} \end{bmatrix} \quad (4)$$

and the blocks of the first level are scalars (1×1 matrices)

$$\mathbf{H}_{m_1, \dots, m_N} = y(m_1, \dots, m_N).$$

By $\tilde{\mathbf{H}}$ we denote the MH matrix constructed from noisy observations \tilde{y} . There are alternative equivalent ways to construct the MH matrix: using selection matrices [7] or using operations with tensors [12].

It can be verified (see [7, Lemma 2] or [12, Section III.A]) that for the noiseless signal the MH matrix admits a factorization of the form

$$\mathbf{H} = \mathbf{P} \text{diag}(\mathbf{c}) \mathbf{Q}^\top \quad (5)$$

where

$$\mathbf{P} = \mathbf{A}_1^{(L_1)} \odot \mathbf{A}_2^{(L_2)} \odot \cdots \odot \mathbf{A}_N^{(L_N)}, \quad \mathbf{Q} = \mathbf{A}_1^{(K_1)} \odot \mathbf{A}_2^{(K_2)} \odot \cdots \odot \mathbf{A}_N^{(K_N)},$$

\odot denotes the Khatri-Rao product, $\mathbf{A}_n^{(L_n)} \in \mathbb{C}^{L_n \times R}$ are Vandermonde matrices (with $(\mathbf{A}_n^{(L_n)})_{j,r} = a_{r,n}^{j-1}$), and $\mathbf{c} = [c_1, \dots, c_R]^\top$ is the vector of amplitudes.

2.2 Shift properties of subspaces

Let us define the selection matrices

$$\mathbf{I}^{\bar{n}} \stackrel{\text{def}}{=} \mathbf{I}_{L_1} \boxtimes \mathbf{I}_{L_2} \boxtimes \cdots \boxtimes \bar{\mathbf{I}}_{L_n} \boxtimes \cdots \boxtimes \mathbf{I}_{L_N} = \mathbf{I}_{\prod_{i=1}^{n-1} L_i} \boxtimes \bar{\mathbf{I}}_{L_n} \boxtimes \mathbf{I}_{\prod_{i=n+1}^N L_i} \quad (6)$$

$$\mathbf{I}^{\underline{n}} \stackrel{\text{def}}{=} \mathbf{I}_{L_1} \boxtimes \mathbf{I}_{L_2} \boxtimes \cdots \boxtimes \underline{\mathbf{I}}_{L_n} \boxtimes \cdots \boxtimes \mathbf{I}_{L_N} = \mathbf{I}_{\prod_{i=1}^{n-1} L_i} \boxtimes \underline{\mathbf{I}}_{L_n} \boxtimes \mathbf{I}_{\prod_{i=n+1}^N L_i} \quad (7)$$

and

$$\underline{\underline{\mathbf{J}}} = \underline{\underline{\mathbf{I}}}_{L_1} \boxtimes \underline{\underline{\mathbf{I}}}_{L_2} \boxtimes \cdots \boxtimes \underline{\underline{\mathbf{I}}}_{L_N}, \quad (8)$$

$$\mathbf{J}_n = \underline{\underline{\mathbf{I}}}_{L_1} \boxtimes \underline{\underline{\mathbf{I}}}_{L_2} \boxtimes \cdots \boxtimes \bar{\mathbf{I}}_{L_n} \boxtimes \cdots \boxtimes \underline{\underline{\mathbf{I}}}_{L_N}, \quad \bar{\bar{\mathbf{J}}} = \sum_{n=1}^N \beta_n \mathbf{J}_n, \quad (9)$$

where $\underline{\underline{\mathbf{X}}}$ (resp. $\bar{\bar{\mathbf{X}}}$) represents \mathbf{X} without the last (resp. first) row, \boxtimes denotes the Kronecker product, and $\underline{\underline{\mathbf{I}}}_L$ is an $L \times L$ identity matrix.

Next, for a matrix \mathbf{X} we define $\overset{n-}{\mathbf{X}} = \overset{n-}{\mathbf{I}} \mathbf{X}$ and $\underset{n}{\mathbf{X}} = \underset{n}{\mathbf{I}} \mathbf{X}$. Then the shifted versions of \mathbf{P} satisfy the following equation:

$$\underset{n}{\mathbf{P}} \boldsymbol{\Psi}_n = \overset{n-}{\mathbf{P}}, \quad (10)$$

where $\boldsymbol{\Psi}_n = \text{diag}(\mathbf{a}_{(n)})$, $\mathbf{a}_{(n)} = [a_{1,n}, \dots, a_{R,n}]^\top$.

Now consider the matrix \mathbf{U}_s of the leading R left singular vectors of the noiseless matrix \mathbf{H} . Since the ranges of \mathbf{U}_s and \mathbf{P} coincide, they are linked by a nonsingular transformation:

$$\mathbf{P} = \mathbf{U}_s \mathbf{T}.$$

Hence, we have that the matrix $\mathbf{F}_n \stackrel{\text{def}}{=} \mathbf{T} \boldsymbol{\Psi}_n \mathbf{T}^{-1}$ satisfies the equation

$$\underset{n}{\mathbf{U}}_s \mathbf{F}_n = \overset{n-}{\mathbf{U}}_s. \quad (11)$$

If $\underset{n}{\mathbf{U}}_s$ is full-column rank, then \mathbf{F}_n can be obtained as:

$$\mathbf{F}_n = (\underset{n}{\mathbf{I}} \underset{n}{\mathbf{U}}_s)^\dagger \left(\overset{n-}{\mathbf{I}} \overset{n-}{\mathbf{U}}_s \right) := \left(\underset{n-}{\mathbf{U}}_s \right)^\dagger \left(\overset{n-}{\mathbf{U}}_s \right) \quad (12)$$

Hence, the matrices \mathbf{F}_n can be computed from the signal subspace \mathbf{U}_s , and the modes of each dimension n can be estimated by the eigenvalues of \mathbf{F}_n .

On the other side it was shown in [6] that

$$\mathbf{G} = \underline{\underline{\mathbf{J}}} \mathbf{U}_s \mathbf{T}, \quad \mathbf{G} \text{Diag}(\boldsymbol{\eta}) = \overline{\overline{\mathbf{J}}} \mathbf{U}_s \mathbf{T}, \quad (13)$$

with $\mathbf{G} = \mathbf{A}_1^{(L_1-1)} \odot \dots \odot \mathbf{A}_N^{(L_N-1)}$, $\boldsymbol{\eta} = [\eta_1, \dots, \eta_R]^\top$ and $\eta_r = \sum_{n=1}^N \beta_n a_{r,n}$ where β_n are user parameters such that $\eta_r \neq \eta_i$ for $r \neq i$.

From (13) it follows that

$$\mathbf{T} \text{Diag}(\boldsymbol{\eta}) \mathbf{T}^{-1} = (\underline{\underline{\mathbf{J}}} \mathbf{U}_s)^\dagger (\overline{\overline{\mathbf{J}}} \mathbf{U}_s), \quad (14)$$

Hence, the modes can be estimated from the elements of \mathbf{G} .

3 ESPRIT-type algorithms for MH matrices

3.1 N-D ESPRIT algorithm

The N-D ESPRIT algorithm [12] is an extension of the 2-D ESPRIT [8] and ESPRIT [9] algorithms. The algorithm consists of the following steps :

1. Choose L_1, \dots, L_N .
2. Construct the MH matrix $\tilde{\mathbf{H}}$ from the noisy signal.
3. Perform the SVD of $\tilde{\mathbf{H}}$, and form the matrix $\tilde{\mathbf{U}}_s \in \mathbb{C}^{(L_1 \cdots L_N) \times R}$ of the R dominant singular vectors.
4. Compute the matrices $\tilde{\mathbf{F}}_n$ such that:

$$\tilde{\mathbf{F}}_n := \left(\tilde{\underset{n}{\mathbf{U}}}_s \right)^\dagger \left(\tilde{\overset{n-}{\mathbf{U}}}_s \right) \quad (15)$$

5. For given parameters β_1, \dots, β_n , compute a linear combination of $\tilde{\mathbf{F}}_n$:

$$\tilde{\mathbf{K}} = \sum_{n=1}^N \beta_n \tilde{\mathbf{F}}_n \quad (16)$$

6. Compute a diagonalizing matrix \mathbf{T} of $\tilde{\mathbf{K}}$ from its EVD:

$$\tilde{\mathbf{K}} = \mathbf{T} \text{Diag}(\boldsymbol{\eta}) \mathbf{T}^{-1}. \quad (17)$$

7. Apply the transformation \mathbf{T} to \mathbf{F}_n :

$$\tilde{\mathbf{D}}_n = \mathbf{T}^{-1} \tilde{\mathbf{F}}_n \mathbf{T}, \quad \text{for } n = 1, \dots, N. \quad (18)$$

8. Extract $\{\hat{a}_{1,n}, \dots, \hat{a}_{R,n}\}_{n=1}^N$ from $\text{diag}(\tilde{\mathbf{D}}_n)$, $n = 1, \dots, N$.

3.2 IMDF algorithm

The IMDF algorithm consists of the following steps [6]:

1. Choose L_1, \dots, L_N .
2. Construct the MH matrix $\tilde{\mathbf{H}}$ from the noisy signal.
3. Perform the SVD of $\tilde{\mathbf{H}}$, and form $\tilde{\mathbf{U}}_s \in \mathbb{C}^{(L_1 \dots L_N) \times R}$, as in N-D ESPRIT.
4. Compute the matrix $\tilde{\mathbf{K}}_{\text{IMDF}} = (\underline{\mathbf{J}} \tilde{\mathbf{U}}_s)^\dagger (\overline{\mathbf{J}} \tilde{\mathbf{U}}_s)$.
5. Compute a diagonalizing matrix \mathbf{T} of $\tilde{\mathbf{K}}_{\text{IMDF}}$ from its EVD:

$$\tilde{\mathbf{K}}_{\text{IMDF}} = \mathbf{T} \text{Diag}(\boldsymbol{\eta}) \mathbf{T}^{-1}. \quad (19)$$

6. Estimate a scaled and permuted matrix $\tilde{\mathbf{G}}$:

$$\tilde{\mathbf{G}} = \underline{\mathbf{J}} \tilde{\mathbf{U}}_s \mathbf{T} \quad (20)$$

7. Extract $\{\hat{a}_{1,n}, \dots, \hat{a}_{R,n}\}_{n=1}^N$ from $\tilde{\mathbf{G}}$ by

$$\hat{a}_{r,n} = \frac{1}{\mu_n} \sum_{\substack{k=1 \\ \text{mod}(k-1, L'_{n-1}) \geq L'_n}}^{L'_0} \frac{\tilde{G}_{k,r}}{\tilde{G}_{k-L'_n,r}}, \quad (21)$$

$$\text{where } \mu_n = \frac{L'_0(L_n-2)}{L_n-1} \text{ and } L'_n = \begin{cases} \prod_{i=n+1}^N (L_i - 1), & 0 \leq n \leq N-1, \\ 1, & n = N. \end{cases}$$

3.3 IMDF based on least squares (IMDF LS)

The averaging (21) may not be optimal, if some elements of $\tilde{\mathbf{G}}$ take small values. To tackle this problem, we propose a modification of IMDF. The algorithm is the same as IMDF, except the last two steps, which are replaced by the following:

6. Estimate the scaled and permuted matrix $\tilde{\mathbf{P}}$

$$\tilde{\mathbf{P}} = [\tilde{\mathbf{p}}_1, \dots, \tilde{\mathbf{p}}_R] = \tilde{\mathbf{U}}_s \mathbf{T}.$$

7. Extract $\{\hat{a}_{1,n}, \dots, \hat{a}_{R,n}\}_{n=1}^N$ from $\tilde{\mathbf{P}}$ as

$$\hat{a}_{r,n} = \frac{(\tilde{\mathbf{p}}_r)^{\text{H}_n^-} \tilde{\mathbf{p}}_r}{\|\tilde{\mathbf{p}}_r\|_2^2} = (\tilde{\mathbf{p}}_r)^{\dagger_n^-} \tilde{\mathbf{p}}_r.$$

4 Perturbation analysis

4.1 Basic expressions

The SVD of the noiseless MH matrix \mathbf{H} is given by:

$$\mathbf{H} = \mathbf{U}_s \boldsymbol{\Sigma}_s \mathbf{V}_s^H + \mathbf{U}_n \boldsymbol{\Sigma}_n \mathbf{V}_n^H, \quad (22)$$

where $\boldsymbol{\Sigma}_n = \mathbf{0}$. The subspace decomposition of the perturbed matrix $\tilde{\mathbf{H}} = \mathbf{H} + \Delta\mathbf{H}$ is given by

$$\tilde{\mathbf{H}} = \tilde{\mathbf{U}}_s \tilde{\boldsymbol{\Sigma}}_s \tilde{\mathbf{V}}_s^H + \tilde{\mathbf{U}}_n \tilde{\boldsymbol{\Sigma}}_n \tilde{\mathbf{V}}_n^H \quad (23)$$

We use the following lemma on the first-order approximation.

Lemma 1 ([4] and [15]). *The perturbed signal subspace is $\tilde{\mathbf{U}}_s = \mathbf{U}_s + \Delta\mathbf{U}_s$, $\tilde{\mathbf{V}}_s = \mathbf{V}_s + \Delta\mathbf{V}_s$ and $\tilde{\boldsymbol{\Sigma}}_s = \boldsymbol{\Sigma}_s + \Delta\boldsymbol{\Sigma}_s$. A first order perturbation is given by*

$$\Delta\mathbf{U}_s = \mathbf{U}_n \mathbf{U}_n^H \Delta\mathbf{H} \mathbf{V}_s \boldsymbol{\Sigma}_s^{-1} \quad (24)$$

$$\Delta\mathbf{V}_s^H = \boldsymbol{\Sigma}_s^{-1} \mathbf{U}_s^H \Delta\mathbf{H} \mathbf{V}_n \mathbf{V}_n^H, \quad \Delta\boldsymbol{\Sigma}_s = \mathbf{U}_s^H \Delta\mathbf{H} \mathbf{V}_s \quad (25)$$

For N-D ESPRIT, an expression for first-order perturbation was derived in [12].

Proposition 1 ([12]). *Denote by $\mathbf{b}_r \in \mathbb{C}^R$ the r -th unit vector. Then first order perturbations of the modes obtained by the N-D ESPRIT admit an expansion*

$$\Delta a_{r,n} = \frac{1}{c_r} \mathbf{b}_r^\top \mathbf{P}^\dagger (\mathbf{I} - a_{r,n} \mathbf{I}) \Delta\mathbf{H} (\mathbf{Q}^\top)^\dagger \mathbf{b}_r. \quad (26)$$

4.2 IMDF Perturbations

Perturbation analysis of IMDF have been done in [6]. However, the obtained expressions require the calculation of the SVD of the MH matrix \mathbf{H} . To get simplified perturbation expressions we use the following fact: from (9), \mathbf{K}_{IMDF} can be written as a linear combination of $\mathbf{F}_n^{\text{IMDF}}$

$$\mathbf{K}_{\text{IMDF}} = \sum_{n=1}^N \beta_n \mathbf{F}_n^{\text{IMDF}}, \quad (27)$$

where

$$\mathbf{F}_n^{\text{IMDF}} = (\underline{\mathbf{J}}\mathbf{U}_s)^\dagger (\mathbf{J}_n \mathbf{U}_s). \quad (28)$$

We use the following lemma, which is a slight modification of [12, Lemma 4].

Lemma 2 ([12, Lemma 4, a modification]). *The first-order perturbation of $\mathbf{F}_n^{\text{IMDF}}$ is given by*

$$\Delta\mathbf{F}_n^{\text{IMDF}} = (\underline{\mathbf{J}}\mathbf{U}_s)^\dagger (\mathbf{J}_n \Delta\mathbf{U}_s - \underline{\mathbf{J}}\Delta\mathbf{U}_s \mathbf{F}_n). \quad (29)$$

Next, we derive perturbation expression of $a_{r,n}$ with respect to $\Delta \mathbf{g}_r$ from (21)

$$\Delta a_{r,n} = \frac{a_{r,n} G_{1,r}^{-1}}{\mu_n} \mathbf{v}_{r,n}^\top \Delta \mathbf{g}_r, \quad (30)$$

where

$$\mathbf{v}_{r,n} = (\phi_{r,1} \boxtimes \cdots \boxtimes \phi_{r,n-1}) \boxtimes \psi_{r,n} \boxtimes (\phi_{r,n+1} \boxtimes \cdots \boxtimes \phi_{r,N}), \quad (31)$$

$$\phi_{r,1} = \begin{bmatrix} 1 & a_{r,n}^{-1} & \cdots & a_{r,n}^{-(L_n-2)} \end{bmatrix}^\top \in \mathbb{C}^{(L_n-1) \times 1}, \quad (32)$$

$$\psi_{r,1} = \begin{bmatrix} -1 & 0 & \cdots & 0 & a_{r,n}^{-(L_n-2)} \end{bmatrix}^\top \in \mathbb{C}^{(L_n-1) \times 1}, \quad (33)$$

the vectors \mathbf{g}_r are

$$\mathbf{g}_r = \underline{\mathbf{J}} \mathbf{U}_s \mathbf{t}_r,$$

and \mathbf{t}_r are the eigenvectors of \mathbf{K}_{IMDF} (the columns of \mathbf{T}):

$$\mathbf{T} = [\mathbf{t}_1, \dots, \mathbf{t}_R].$$

The perturbation of \mathbf{g}_r can be expressed as:

$$\Delta \mathbf{g}_r = \underline{\mathbf{J}} \Delta \mathbf{U}_s \mathbf{t}_r + \underline{\mathbf{J}} \mathbf{U}_s \Delta \mathbf{t}_r, \quad (34)$$

where:

- $\Delta \mathbf{U}_s$ can be found from equation (24);
- $\Delta \mathbf{t}_r$ can be found as

$$\Delta \mathbf{t}_r = \sum_{i=1, i \neq r}^R \frac{1}{\eta_r - \eta_i} \mathbf{t}_i \boldsymbol{\tau}_i^\top \Delta \mathbf{K} \mathbf{t}_r \quad (35)$$

$$= \mathbf{T} \boldsymbol{\Xi}(r) \mathbf{T}^{-1} \Delta \mathbf{K} \mathbf{t}_r. \quad (36)$$

where $\boldsymbol{\tau}_r^\top$ denote the rows of \mathbf{T}^{-1}

$$\mathbf{T}^{-1} = [\boldsymbol{\tau}_1, \dots, \boldsymbol{\tau}_R]^\top,$$

and $\boldsymbol{\Xi}(r)$ is a diagonal matrix with $\boldsymbol{\Xi}_{ii}(r) = \frac{1}{\eta_r - \eta_i}$, for $i \neq r$ and $\boldsymbol{\Xi}_{rr}(r) = 0$.

From equations (27), (28), and (35) we get, after some simplifications

$$\begin{aligned} \Delta \mathbf{t}_r = \sum_{n=1}^N \beta_n \left\{ \mathbf{T} \boldsymbol{\Xi}(r) \mathbf{P}^\dagger (\mathbf{J}_n - a_{r,n} \underline{\mathbf{J}}) + \right. \\ \left. \sum_{i=1, i \neq r}^R \frac{(a_{r,n} - a_{i,n})}{\eta_r - \eta_i} \mathbf{t}_i \boldsymbol{\tau}_i^\top (\mathbf{T}^{-1})^\mathbf{H} \mathbf{P}^\mathbf{H} \right\} \frac{1}{c_r} \Delta \mathbf{H} (\mathbf{Q}^\top)^\dagger \mathbf{b}_r. \end{aligned} \quad (37)$$

Then, by combining (24) and (37), we get

$$\Delta \mathbf{g}_r = \underline{\mathbf{J}} \left\{ (\mathbf{I} - \mathbf{P} \mathbf{b}_r \mathbf{b}_r^\top \mathbf{P}^\dagger) + \mathbf{P} \boldsymbol{\Xi}(r) \mathbf{P}^\dagger (\underline{\mathbf{J}} - \eta_r \underline{\mathbf{J}}) \right\} \cdot \frac{1}{c_r} \Delta \mathbf{H} (\mathbf{Q}^\top)^\dagger \mathbf{b}_r. \quad (38)$$

Here the SVD of \mathbf{H} is not required.

4.3 IMDF LS perturbations

For establishing the perturbations of $a_{r,n}$ for IMDF LS we can use eqn. (29):

$$\Delta a_{r,n} = (\underline{\mathbf{p}}_r)^\dagger (\Delta \underline{\mathbf{p}}_r - \Delta \underline{\mathbf{p}}_r a_{r,n}) = \frac{1}{\|\underline{\mathbf{p}}_r\|_2^2} \underline{\mathbf{p}}_r^H (\mathbf{J}_n - a_{r,n} \underline{\mathbf{J}}) \Delta \underline{\mathbf{p}}_r$$

The perturbation $\Delta \underline{\mathbf{p}}_r$ is, in fact, given in (34). Finally, since

$$(\mathbf{J}_n - a_{r,n} \underline{\mathbf{J}}) \mathbf{P} \mathbf{b}_r = 0,$$

we have

$$\Delta a_{r,n} = \frac{1}{c_r \|\underline{\mathbf{p}}_r\|_2^2} \underline{\mathbf{p}}_r^H (\mathbf{J}_n - a_{r,n} \underline{\mathbf{J}}) \left(\mathbf{I} + \mathbf{P} \underline{\boldsymbol{\Xi}}(r) \underline{\mathbf{P}}^\dagger \left(\overline{\mathbf{J}} - \eta_r \underline{\mathbf{J}} \right) \right) \Delta \mathbf{H} (\mathbf{Q}^\top)^\dagger \mathbf{b}_r. \quad (39)$$

4.4 Computing the first-order perturbation and its moments

Similarly to [12, §V.C], the perturbations in eqn. (26), (38), (39) have the common form:

$$\Delta a_{r,n} = \mathbf{v}_{r,n}^\top \Delta \mathbf{H} \mathbf{x}_r,$$

where $\mathbf{x}_r = (\mathbf{Q}^\top)^\dagger \mathbf{b}_r$, and the vector $\mathbf{v}_{r,n}^\top$ depends on the method. Since the MH matrix $\Delta \mathbf{H}$ depends linearly on the elements of \mathbf{e} (vectorization of the noise term), the perturbation can be expressed as

$$\Delta a_{r,n} = \mathbf{z}_{r,n}^H \mathbf{e}. \quad (40)$$

where $\mathbf{z}_{r,n}$ can be computed from $\mathbf{v}_{r,n}^\top$ and \mathbf{x}_r efficiently using the N-D convolution, as shown in [12].

Therefore, we have the following:

1. $\mathbb{E} \{ \Delta a_{r,n} \} = 0$ if \mathbf{e} is zero-mean.
2. $\mathbb{E} \{ \Delta a_{r,n}^2 \} = 0$ if \mathbf{e} is circular.
3. $\mathbb{E} \{ |\Delta a_{r,n}|^2 \} = \mathbf{z}_{r,n}^H \Gamma \mathbf{z}_{r,n}$ if \mathbf{e} has covariance matrix $\Gamma = \mathbb{E} \{ \mathbf{e} \mathbf{e}^H \}$.
4. $\mathbb{E} \{ |\Delta a_{r,n}|^2 \} = \sigma_e^2 \|\mathbf{z}_{r,n}\|_2^2$ if \mathbf{e} is white with variance σ_e^2 .
5. Finally,

$$\text{var}(\Delta \omega_{r,n}) = \text{var}(\Delta \alpha_{r,n}) = \frac{\mathbb{E} \{ |\Delta a_{r,n}|^2 \}}{2|a_{r,n}|^2}$$

if \mathbf{e} is complex circular Gaussian.

5 Simulations

Numerical simulations have been carried out to verify theoretical expressions and compare the performances of N-D ESPRIT, IMDF and IMDF LS algorithms in the presence of white Gaussian noise. The performances are measured by the total mean squared error (tmSE) on estimated parameters. The total MSE is

defined as $\text{tMSE}_{\text{total}} = \frac{1}{RF} \mathbb{E}_p \left\{ \sum_{r=1}^R \sum_{f=1}^F (\xi_{f,r} - \hat{\xi}_{f,r})^2 \right\}$ where $\hat{\xi}_{f,r}$ is an estimate of $\xi_{f,r}$, and \mathbb{E}_p is the average over p Monte-Carlo trials. In our simulations, $\xi_{f,r}$ can be either a frequency or a damping factor.

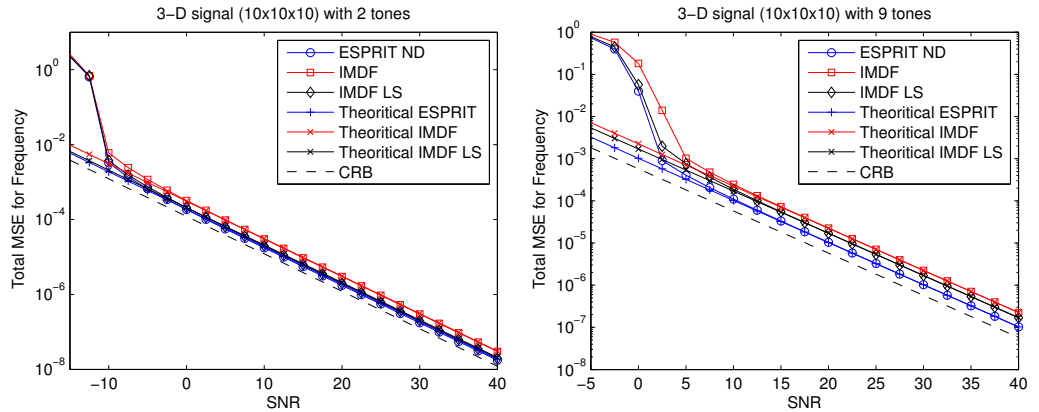
In the following experiments we plot theoretical expressions of the variances and compare them with empirical results of N-D ESPRIT, IMDF and IMDF LS. Cramér-Rao bounds are also reported [11]. In all experiments, $L_n = \lceil \frac{M_n}{3} \rceil$.

Experiment 1 In this experiment, we simulate a 3-D signal of size $10 \times 10 \times 10$ containing two modes whose parameters are given in Table 1. Figure 1(a) shows the obtained results. We can see that N-D ESPRIT and IMDF LS have the similar results, which are almost equal to theoretical ones beyond -10 dB. We can also remark that N-D ESPRIT and IMDF LS outperforms slightly IMDF.

Table 1. 3-D signal with two modes

r	$\omega_{r,1}$	$\alpha_{r,1}$	$\omega_{r,2}$	$\alpha_{r,2}$	$\omega_{r,3}$	$\alpha_{r,3}$	c_r
1	0.2π	0.01	0.3π	0.01	0.26π	0.01	1
2	0.6π	0.01	0.8π	0.015	0.2π	0.01	1

Experiment 2 In this experiment, we simulate a 3-D signal of size $10 \times 10 \times 10$ containing nine modes. Figure 1(b) shows the obtained results. First, we remark that theoretical variances match the empirical ones beyond thresholds. Then, we can see that N-D ESPRIT outperforms IMDF and IMDF LS.



(a) 3-D damped signal containing two tones. (b) 3-D damped signal containing nine tones.

Fig. 1. Theoretical and empirical tMSEs versus SNR. $(M_1, M_2, M_3) = (10, 10, 10)$.

6 Conclusions

Our study suggests that the N-D ESPRIT outperforms IMDF when the number of tones increases. The same conclusion holds for the improvement of IMDF proposed in this paper. We conjecture that the eigenvalue-based estimation should be preferred over the eigenvector-based ones, since they do not contain an additional estimation step. An extensive study (for different noise scenarios and parameter values of the methods) is needed to confirm our conjecture.

References

1. Gershman, A.B., Sidiropoulos, N.D.: Space-time processing for MIMO communications. Wiley Online Library (2005)
2. Haardt, M., Roemer, F., Del Galdo, G.: Higher-order SVD-based subspace estimation to improve the parameter estimation accuracy in multidimensional harmonic retrieval problems. *IEEE Trans. Signal Process.* 56(7), 3198–3213 (2008)
3. Hua, Y.: Estimating two-dimensional frequencies by matrix enhancement and matrix pencil. *IEEE Trans. Signal Process.* 40(9), 2267–2280 (1992)
4. Li, F., Liu, H., Vaccaro, R.J.: Performance analysis for DOA estimation algorithms: unification, simplification, and observations. *IEEE Trans. Aerosp. Electron Syst.* 29(4), 1170–1184 (1993)
5. Li, Y., Razavilar, J., Liu, K.: A high-resolution technique for multidimensional NMR spectroscopy. *IEEE Trans. Biomed. Eng.* 45(1), 78–86 (1998)
6. Liu, J., Liu, X., Ma, X.: Multidimensional frequency estimation with finite snapshots in the presence of identical frequencies. *IEEE Trans. Signal Process.* 55, 5179–5194 (2007)
7. Liu, J., Liu, X.: An eigenvector-based approach for multidimensional frequency estimation with improved identifiability. *IEEE Trans. Signal Process.* 54(12), 4543–4556 (2006)
8. Rouquette, S., Najim, M.: Estimation of frequencies and damping factors by two-dimensional ESPRIT type methods. *IEEE Trans. Signal Process.* 49(1), 237–245 (2001)
9. Roy, R., Kailath, T.: ESPRIT-estimation of signal parameters via rotational invariance techniques. *IEEE Trans. Acoust., Speech and Signal Process.* 37(7), 984–995 (1989)
10. Sacchini, J., Steedly, W., Moses, R.: Two-dimensional Prony modeling and parameter estimation. *IEEE Trans. Signal Process.* 41(11), 3127–3137 (1993)
11. Sahnoun, S., Djermoune, E.H., Brie, D., Comon, P.: A simultaneous sparse approximation method for multidimensional harmonic retrieval. *Signal Processing* 137, 36–48 (2017)
12. Sahnoun, S., Usevich, K., Comon, P.: Multidimensional ESPRIT: Algorithm, computations and perturbation analysis. Tech. rep. (2016), hal-01360438
13. So, H.C., Chan, F., Lau, W., Chan, C.F.: An efficient approach for two-dimensional parameter estimation of a single-tone. *IEEE Trans. Signal Process.* 58(4), 1999–2009 (2010)
14. Sun, W., So, H.C.: Accurate and computationally efficient tensor-based subspace approach for multidimensional harmonic retrieval. *IEEE Trans. Signal Process.* 60(10), 5077–5088 (2012)
15. Xu, Z.: Perturbation analysis for subspace decomposition with applications in subspace-based algorithms. *IEEE Trans. Signal Process.* 50(11), 2820–2830 (2002)